

Bose-Einstein condensate in a double-well potential as an open quantum system

Janne Ruostekoski and Dan F. Walls

Department of Physics, University of Auckland, Private Bag 92019, Auckland, New Zealand

(October 11, 2018)

We study the dynamics of a Bose-Einstein condensate in a double-well potential in the two-mode approximation. The dissipation of energy from the condensate is described by the coupling to a thermal reservoir of non-condensate modes. As a consequence of the coupling the self-locked population imbalance in the macroscopic quantum self-trapping decays away. We show that a coherent state predicted by spontaneous symmetry breaking is not robust and decoheres rapidly into a statistical mixture due to the interactions between condensate and non-condensate atoms. However, via stochastic simulations we find that with a sufficiently fast measurement rate of the relative phase between the two wells the matter wave coherence is established even in the presence of the decoherence.

03.75.Fi,42.50.Vk,05.30.Jp,03.65.Bz

Bose-Einstein condensates (BEC's) exhibit a macroscopic quantum coherence which in thermal atomic ensembles is absent [1]. In the conventional reasoning the BEC is assigned a macroscopic wave function with an arbitrary but fixed phase. The selection of a phase implies the spontaneous breaking of the gauge symmetry. The atom-atom interactions in finite-sized BEC's affect coherence properties. The relative phase of BEC's undergoes diffusion or collapses due to the condensate self-interactions [2,3]. The interactions between condensate and non-condensate atoms create decoherence [4]. Modelling decoherence by fully including the quantum effects requires sophisticated theoretical studies which non-trivially include non-condensate atoms. In the experiments on BEC's of dilute alkali atomic gases [5] trapped atoms are evaporatively cooled and continuously exchange particles with their environment. Thus, standard approaches of quantum optics for open systems involving master equations and heat reservoirs seem especially natural for treating atomic BEC's [6–10].

In this paper we study the evolution of the master equation for a BEC in a double-well potential in a two-mode approximation using previously derived models [7]. Macroscopic quantum coherence of BEC's results in coherent quantum tunneling of atoms between the two modes or the “two BEC's”, which is analogous to the coherent tunneling of Cooper pairs in a Josephson junction [11–15]. According to the Josephson effect, the atom numbers of the BEC's oscillate even if the number of atoms in each condensate is initially equal. Even BEC's with a well-defined number of atoms, and with no phase information, could exhibit oscillations in particular mea-

surement processes on atoms [16] or on photons [17,18].

One interesting feature of the coherent quantum tunneling between two BEC's is that due to the nonlinearity arising from atom-atom interactions, oscillations are expected to be suppressed when the population difference exceeds a critical value in a process known as macroscopic quantum self-trapping (MQST) [13,14]. We show that in the presence of collisions between the condensate and non-condensate atoms MQST decays away, i.e., the atom numbers of the two BEC's become balanced.

Anglin [7] derived the master equation for a trapped BEC by considering a special model of a BEC confined in a deep but narrow spherical square-well potential, tuned so as to possess exactly one single-particle bound state. In this model the thermal reservoir of non-condensate atoms consists of a continuum of unbound modes obtained by the scattering solutions of the potential well. The binding energy E_b of the BEC mode is assumed to be large compared to the thermal energy of the non-condensed atoms. Then the fugacity satisfies $z = e^{\beta\mu} \ll 1$, where μ is the chemical potential and $\beta = 1/(k_B T)$, even in the presence of a BEC. The condensation occurs because of the depth of the attractive potential. The small fugacity allows the derivation of the master equation in the Markov and Born approximations. By expanding in terms of the small parameters z and a/d , where a is the s -wave scattering length and d is the length scale of the BEC, the reduced density operator for the BEC satisfies the following equation of motion:

$$\dot{\rho} = i/\hbar[\rho, H_S] + C_1 \mathcal{D}[b^\dagger b]\rho + C_2 \mathcal{D}[b^\dagger]\rho + C_2 \exp\{\beta(\hbar\Delta - \mu)/2\} \mathcal{D}[b]\rho + \mathcal{O}(z^2 a^3/d^3). \quad (1)$$

Here we have defined

$$\mathcal{D}[c]\rho \equiv c\rho c^\dagger - 1/2(c^\dagger c\rho + \rho c^\dagger c), \quad (2)$$

and $\Delta \simeq 2\kappa N - E_b$ is expressed in terms of the strength of the self-interaction energy κ . The system Hamiltonian for the BEC is denoted by H_S . For simplicity, the interactions between different non-condensate atoms are estimated by the Boltzmann scattering rate $\gamma = \sigma n\hbar k/m$, where σ is the scattering cross-section and n is the density of the gas. The parameters C_1 and C_2 may then be estimated by $C_1 \sim \gamma$ and $C_2/C_1 \simeq z/(\beta E_b)$.

In a single mode approximation the processes in which a BEC atom collides with a non-condensate atom and produces two BEC particles, or vice versa, do not conserve the energy and they are absent in Eq. (1). The term proportional to C_1 describes elastic two-body collisions between condensate and non-condensate atoms and

it induces phase decoherence [19]. Inelastic collisions [the terms proportional to C_2 in Eq. (1)] introduce amplitude decoherence [19]. With the present approximations the amplitude decoherence is dramatically reduced compared to the phase damping. The central assumption is a small fugacity indicating $\beta E_b \gg 1$. In the scattering processes the energy must be conserved to leading order, so that depletion and growth of the BEC involve non-condensate atoms with high enough energy to balance the large binding energy of the trapped state. If the BEC is described by a multiple number of modes [8], the amplitude decoherence does not need to be small compared to the phase decoherence. The necessary condition for the validity of the single-mode approximation in a harmonic trap is that the self-energy of the atom-atom interactions of the BEC should not dominate over the mode energy spacing. This assumption clearly breaks down in the Thomas-Fermi limit in which the kinetic energy is negligible compared to the self-interaction energy indicating $(15Na/l)^{1/5} \gg 1$, where $l = (\hbar/m\omega)^{1/2}$ is the length scale of the harmonic oscillator. Jaksch *et al.* [9] have calculated the intensity and the amplitude fluctuations of a BEC. They have evaluated the coefficients of the master equation in the Thomas-Fermi limit and have obtained stronger amplitude decoherence than phase decoherence. Nevertheless, the calculations of the BEC fluctuations are still performed in the one-mode approximation.

We consider Anglin's model for the master equation [7] in the studies of the coherent quantum tunneling of a BEC in a double-well potential. To obtain the system Hamiltonian for the BEC we approximate the total field operator by the two lowest quantum modes and write $\psi(\mathbf{r}) \simeq \phi_b(\mathbf{r})b + \phi_c(\mathbf{r})c$, where ϕ_b and ϕ_c are the local mode solutions of the individual wells with small spatial overlap and the corresponding annihilation operators are b and c . This requires that the BEC self-interaction energy should not dominate over the energy separation of these modes from the higher excited modes. The Hamiltonian in the two-mode approximation reads [13]

$$H_S/\hbar = \xi b^\dagger b + \Omega(b^\dagger c + c^\dagger b) + \kappa[(b^\dagger)^2 b^2 + (c^\dagger)^2 c^2]. \quad (3)$$

Here ξ is the energy difference between the modes. The tunneling between the two wells is described by Ω , which is proportional to the overlap of the spatial mode function of the opposite wells. The short-ranged two-body interaction strength is obtained from $\kappa = 2\pi a\hbar/m \int |\phi_b(\mathbf{r})|^4$, where we have assumed $\int |\phi_b(\mathbf{r})|^4 = \int |\phi_c(\mathbf{r})|^4$.

It is useful to describe the dynamics of Eq. (3) in terms of the atomic coherent states [20], which exhibit coherence, but conserve the total number of atoms:

$$|\theta, \phi\rangle = \sum_{m=-j}^j \binom{2j}{m+j} \frac{\tau^{m+j}}{(1+|\tau|^2)^j} |j, m\rangle, \quad (4)$$

where $|j, m\rangle$ is an eigenstate of the angular momentum operators \hat{J}_z and \hat{J}^2 with eigenvalues m and $j(j+1)$. Here $\tau \equiv e^{-i\phi} \tan(\theta/2)$. We define the angular momentum

operators in terms of the BEC operators in the usual way: $\hat{J}_x = (b^\dagger c + c^\dagger b)/2$, $\hat{J}_y = (b^\dagger c - c^\dagger b)/(2i)$, and $\hat{J}_z = (b^\dagger b - c^\dagger c)/2$. Then $j = N/2$ is a constant of motion and the atomic coherent states may be expressed in terms of the number states of the BEC's

$$|\theta, \phi\rangle_N = \sqrt{\frac{N!}{N^N}} \sum_{l=0}^N \frac{\mathcal{C}^{N-l} \mathcal{B}^l}{\sqrt{l!(N-l)!}} |l, N-l\rangle, \quad (5)$$

where $l = m + N/2$, and \mathcal{B} and \mathcal{C} are the 'coherent amplitudes' of the two BEC's: $\langle b^\dagger b \rangle = |\mathcal{B}|^2$, $\langle c^\dagger c \rangle = |\mathcal{C}|^2$, and $\langle b^\dagger c \rangle = |\mathcal{B}||\mathcal{C}|e^{i\varphi}$. The relative phase between the two wells is φ . Equation (5) clearly shows how the atomic coherent states are projections of the coherent states $|\mathcal{B}, \mathcal{C}\rangle$ onto the basis sets of a fixed total number of atoms N .

We study the evolution of atomic coherent states in the presence of decoherence in both wells b and c . As already noted, with the present approximations the amplitude decoherence is much weaker than the phase decoherence. It is also easy to verify numerically that the coherent states are much less robust for the phase decoherence than for the amplitude decoherence, even if the magnitude of the phase and the amplitude damping is equal. This is also well known in quantum optics [19]. Hence, the effects of the amplitude decoherence are negligible compared to the phase decoherence.

The dynamics of the master equation is studied in terms of stochastic trajectories of state vectors [21]. The master equation is unraveled by Monte-Carlo evolution of wave functions.

In Fig. 1a) we have plotted the expectation value of the number of atoms in the well b , $N_b(t)$. The initial state is the atomic coherent state with the relative phase $\varphi = \pi/2$ between the two wells and the expectation values for the atom numbers $N_b = N_c = 50$. We have set $N\kappa/\Omega = 0.5$ and $\xi = 0$. The solid line is the result without decoherence $\gamma = 0$. The oscillations are damped due to the collapse of the macroscopic coherence [13]. The dashed line has $\gamma = 0.1\kappa$ and the dashed-dotted line $\gamma = 0.4\kappa$. The decoherence clearly increases the damping of the oscillations. Although the model used is very simplified, we can make rough estimates for the parameters. For the effective mode volume $1/\int |\phi(\mathbf{r})|^4 = 10^{-9} \text{ cm}^3$, $a = 5 \text{ nm}$, for ^{23}Na , and for the temperature $T = 100 \text{ nK}$, $\gamma = 0.1\kappa$ corresponds to the density of the non-condensate atoms $n \sim 10^9 \text{ cm}^{-3}$ and the fugacity $z \sim 10^{-3}$. In Fig. 1b) we have plotted $\text{Tr}(\rho^2)$ for the same run of simulations. We see that a pure state predicted by spontaneous symmetry breaking is not robust and decoheres rapidly into a statistical mixture due to the interactions between condensate and non-condensate atoms.

If the nonlinearity is large compared to the tunneling frequency and the population imbalance exceeds a critical value, the oscillations of the atom numbers are suppressed [13,14]. A large number of atoms remains "locked" in one of the wells. In Fig. 2a) we have plotted $N_b(t)$ obtained by integrating Eq. (3) (the solid line) and the solution of the master equation in the presence

of the decoherence $\gamma = 0.2\kappa$ (the dashed line). In this case $N\kappa/\Omega = 4.5$, $\xi = 0.005\Omega$, and the initial state is the atomic coherent state with the expectation values $N_b = 4N_c = 80$ and $\varphi = 0$. Due to the interactions between condensate and non-condensate atoms MQST vanishes and the atom population becomes balanced.

Next, we include the effect of measurements into the calculations. We assume that the number of atoms is nondestructively measured in one of the two wells. The effect of the measurement is included in quantum trajectory simulations by averaging over the dissipation channels corresponding to the interactions between condensate and non-condensate atoms, but at the same time by considering the measurement of the number of atoms in one of the wells to be a single realization of a stochastic trajectory. We consider a particular situation in which the Josephson dynamics is nondestructively measured by shining a coherent light beam through one of the BEC's.

We assume that the incoming light field with a large detuning from the atomic resonance is scattered from the well b . For instance, if the shape of the gas is flat and the light is shined through a thin dimension, the dipole shifts are small and the sample can be considered optically thin [22]. A BEC atom scatters back to the BEC via coherent spontaneous scattering, stimulated by a large number of atoms in the BEC. Coherently scattered photons are emitted into a narrow cone in the forward direction. The amplitude of the scattered field has the dependence $|\mathbf{E}_S^+| \propto \mathcal{E}d_{eg}/(\hbar\Delta)b^\dagger b$ on the detuning Δ , the dipole matrix element d_{eg} , and the amplitude of the incoming field \mathcal{E} [22]. The direct counting of spontaneously emitted photons can be simulated in terms of quantum trajectories [21], in which the stochastic quantum ‘‘jumps’’ correspond to the detections of photons. The procedure is similar to Ref. [23]. The detection rate of the scattered photons in the present case is $\Gamma\langle(b^\dagger b)^2\rangle \propto |\mathbf{E}_S^- \cdot \mathbf{E}_S^+|$.

If the number of atoms in a BEC is not large, the scattering between the condensate and non-condensate modes is not negligible. This introduces amplitude decoherence similar to the amplitude decoherence due to the atomic collisions in Eq. (1). If we require that the two-mode approximation describes accurately the tunneling dynamics, for small harmonic traps the amplitude decoherence due to the light scattering may not be negligible. For large traps the two-mode approximation can be accurate even for large atom numbers as the BEC self-interaction energy $\kappa \propto l^{-3}$ and the trap frequency $\omega \propto l^{-2}$. Nevertheless, as a first approximation we ignore the decoherence due to the light scattering.

The density matrix of a BEC may be reconstructed by the nondestructive measurements of the number of atoms in one of the wells. The procedure is similar to Ref. [24], except that the density matrix has now time dynamics determined by the Hamiltonian (3), the dissipation, and the back-action of the measurements. Following the notation of Ref. [24], at the time t we have $\rho(t) = \hat{U}(t)^\dagger \rho \hat{U}(t)$, where $\hat{U}(t)$ is in this case the time propagator. Then the

probability of the measurement result of m atoms in the well b at the time t is given by $P_m(t) = \langle m|\rho(t)|m\rangle$. By inverting this expression the density matrix can be reconstructed [24].

The off-diagonal long range order (ODLRO) between the two wells may be described by the visibility of the interference β [17]. To emphasize the effect of decoherence on β we ignore the oscillating dynamics of H_S (including the collapses and revivals) by propagating back the system dynamics. In accordance with Ref. [17] we define

$$\beta e^{i\varphi} \equiv \frac{2}{N} \text{Tr}[e^{iH_S t/\hbar} \rho e^{-iH_S t/\hbar} b^\dagger(0)c(0)]. \quad (6)$$

For a coherent state we have $\beta = 1$, and φ is the relative phase between the two wells. However, for a number state there is no phase information and $\beta = 0$. If the BEC's have unequal atom numbers, the maximum visibility is reduced from one to $\beta_{\max} = 2\sqrt{N_b N_c}/N$. Hence, it is useful to define the relative visibility by $\beta_r \equiv \beta/\beta_{\max}$.

We simulate the dynamics of the dissipation and the measurements by repeating single realizations of quantum trajectories. In the first realization we save the stochastic times of the photon detections. In every subsequent run of the trajectory the times of the photon detections are forced to be the same as in the first run. Although the photon detection times after the first trajectory are deterministic, the collision times between condensate and non-condensate atoms corresponding to the dissipation channels are stochastic in every run. Averaging over all the trajectories allows us to consider the photon measurements to be a ‘‘single realization’’ of the quantum trajectory even though the atomic collisions are at the same time ensemble averages corresponding to the density matrix evolution.

We consider a situation that the two BEC's are initially in pure number states with $N_b = 52$ and $N_c = 48$. We have set $N\kappa/\Omega = 0.25$, $\xi = 0.005\Omega$, and the photon scattering rate $\Gamma = 0.8\kappa$. In Fig. 3a) we have plotted $\beta_r(t)$. The solid line is the result without decoherence $\gamma = 0$. The dashed line has $\gamma = 0.05\kappa$ and the dashed-dotted line $\gamma = 1.8\kappa$. In the beginning for the number state $\beta_r = 0$, but $\beta_r \rightarrow 1$ rapidly even in the presence of weak decoherence. As a consequence of the decoherence ODLRO starts decreasing, but the measurements of spontaneously scattered photons establish the macroscopic coherence, even though the BEC's are initially in pure number states. In Fig. 3b) we have plotted $\text{Tr}(\rho^2)$ for the same run. We see that $\text{Tr}(\rho^2)$ remains close to one and the state is reasonably pure due to the fast measurement rate even in the presence of decoherence if $\gamma = 0.0625\Gamma$. In the case of stronger decoherence with $\gamma = 2.25\Gamma$ the state evolves into a statistical mixture.

In conclusion, we have shown that as a consequence of the interactions between condensate and non-condensate atoms MQST decays away. Due to the interactions a BEC does not remain in a pure state with a well-defined relative phase. However, the coherence properties can be established via the measurement process even in the

presence of decoherence. In particular, nondestructive detections allow the measurements of phase dynamics.

We acknowledge discussions with A. C. Doherty. This work was supported by the Marsden Fund of the Royal Society of NZ and The University of Auckland Research Fund.

FIG. 1. The expectation value of the number of atoms in the well b in a) as a function of time. Initial state is the atomic coherent state with $N_b = N_c = 50$ and the relative phase $\varphi = \pi/2$. The solid line is the result without decoherence $\gamma = 0$. The dashed line has $\gamma = 0.1\kappa$ and the dashed-dotted line $\gamma = 0.4\kappa$. In b) $\text{Tr}(\rho^2)$ for the same run.

FIG. 2. The expectation value of the number of atoms in the well b in the case of large nonlinearity. Initial state is the atomic coherent state with $N_b = 4N_c = 80$ and $\varphi = 0$. The solid line is the result without decoherence and describes the macroscopic quantum self-trapping. The oscillations undergo collapses and revivals. The dashed line shows how the atom population becomes balanced in the presence of decoherence.

FIG. 3. The relative visibility of the interference $\beta_r(t)$ in a) when the number of atoms in one well is nondestructively measured by light scattering. The BEC's are initially in pure number states with $N_b = 52$ and $N_c = 48$. The photon scattering rate $\Gamma = 0.8\kappa$. The solid line is the result without decoherence $\gamma = 0$. The dashed line has $\gamma = 0.05\kappa$ and the dashed-dotted line $\gamma = 1.8\kappa$. In b) $\text{Tr}(\rho^2)$ for the same run.

- [14] A. Smerzi *et al.*, Phys. Rev. Lett. **79**, 4950 (1997).
- [15] I. Zapata, F. Sols, and A. J. Leggett, Phys. Rev. A **57** R28 (1998).
- [16] M. W. Jack, M. J. Collett, and D. F. Walls, Phys. Rev. A **54**, R4625 (1996).
- [17] J. Ruostekoski and D. F. Walls, Phys. Rev. A **56**, 2996 (1997).
- [18] J. F. Corney and G. J. Milburn, cond-mat/9712282.
- [19] D. F. Walls and G. J. Milburn, Phys. Rev. A **31**, 2403 (1985).
- [20] F. T. Arecchi *et al.*, Phys. Rev. A **6**, 2211 (1972).
- [21] J. Dalibard, Y. Castin, and K. Mølmer, J. Opt. Soc. Am. **10**, 524 (1993) and references therein.
- [22] J. Javanainen and J. Ruostekoski, Phys. Rev. A **52**, 3033 (1995).
- [23] J. Ruostekoski *et al.*, Phys. Rev. A **57**, 511 (1998).
- [24] E. L. Bolda, S. M. Tan, and D. F. Walls, Phys. Rev. Lett. **79**, 4719 (1997); R. Walser, *ibid.*, 4724 (1997).

-
- [1] M. R. Andrews *et al.*, Science **275**, 637 (1997); E. A. Burt *et al.*, Phys. Rev. Lett. **79**, 337 (1997).
 - [2] E. M. Wright *et al.*, Phys. Rev. A **56**, 591 (1997).
 - [3] M. Lewenstein and L. You, Phys. Rev. Lett. **77**, 3489 (1996); Y. Castin and J. Dalibard, Phys. Rev. A **55**, 4330 (1997); J. Javanainen and M. Wilkens, Phys. Rev. Lett. **78**, 4675 (1997).
 - [4] W. H. Zurek, Phys. Today **44** (10), 36 (1991) and references therein.
 - [5] M. H. Anderson *et al.*, Science **269**, 198 (1995); K. B. Davis *et al.*, Phys. Rev. Lett. **75**, 3969 (1995); C. C. Bradley *et al.*, Phys. Rev. Lett. **78**, 985 (1997).
 - [6] D. Jaksch, C. W. Gardiner, and P. Zoller, Phys. Rev. A **56**, 575 (1997).
 - [7] J. Anglin, Phys. Rev. Lett. **79**, 6 (1997).
 - [8] C. W. Gardiner and P. Zoller, cond-mat/9712002.
 - [9] D. Jaksch *et al.*, cond-mat/9712206.
 - [10] H. M. Wiseman and J. A. Vacaro, unpublished.
 - [11] J. Javanainen, Phys. Rev. Lett. **57**, 3164 (1986).
 - [12] F. Dalfovo, L. Pitaevskii, and S. Stringari, Phys. Rev. A **54**, 4213 (1996).
 - [13] G. J. Milburn *et al.*, Phys. Rev. A **55**, 4318 (1997).

Fig.1a

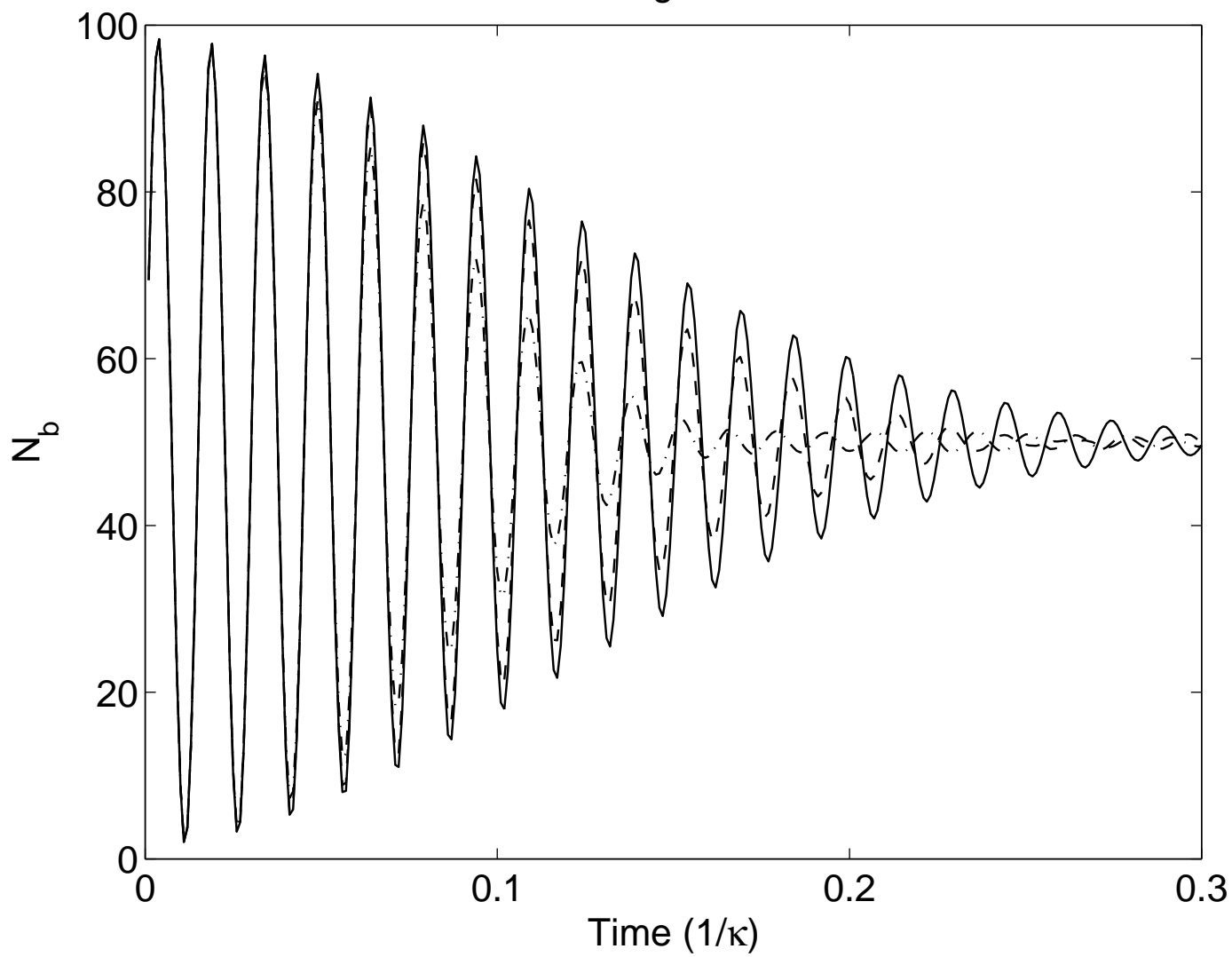


Fig.1b

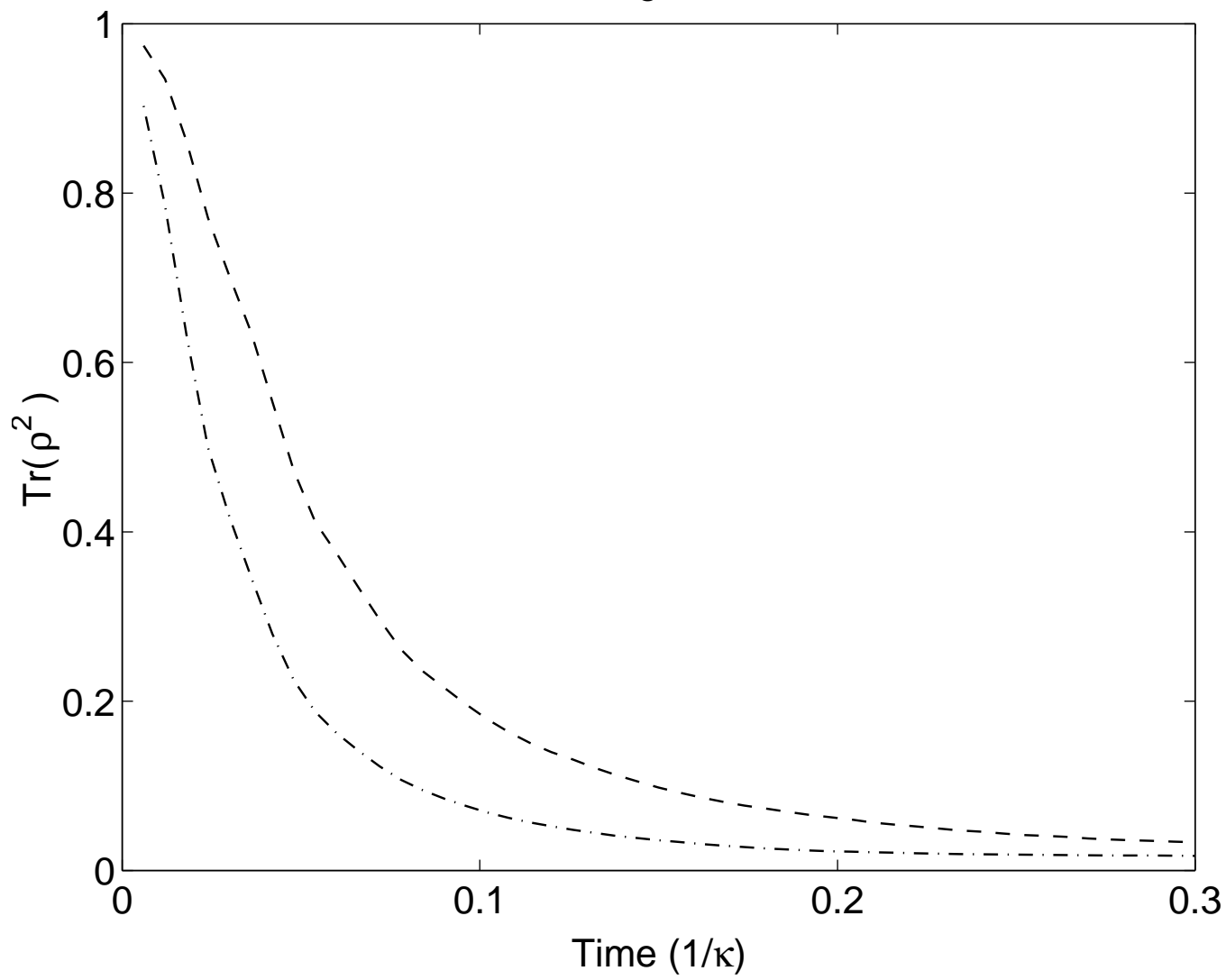


Fig.2

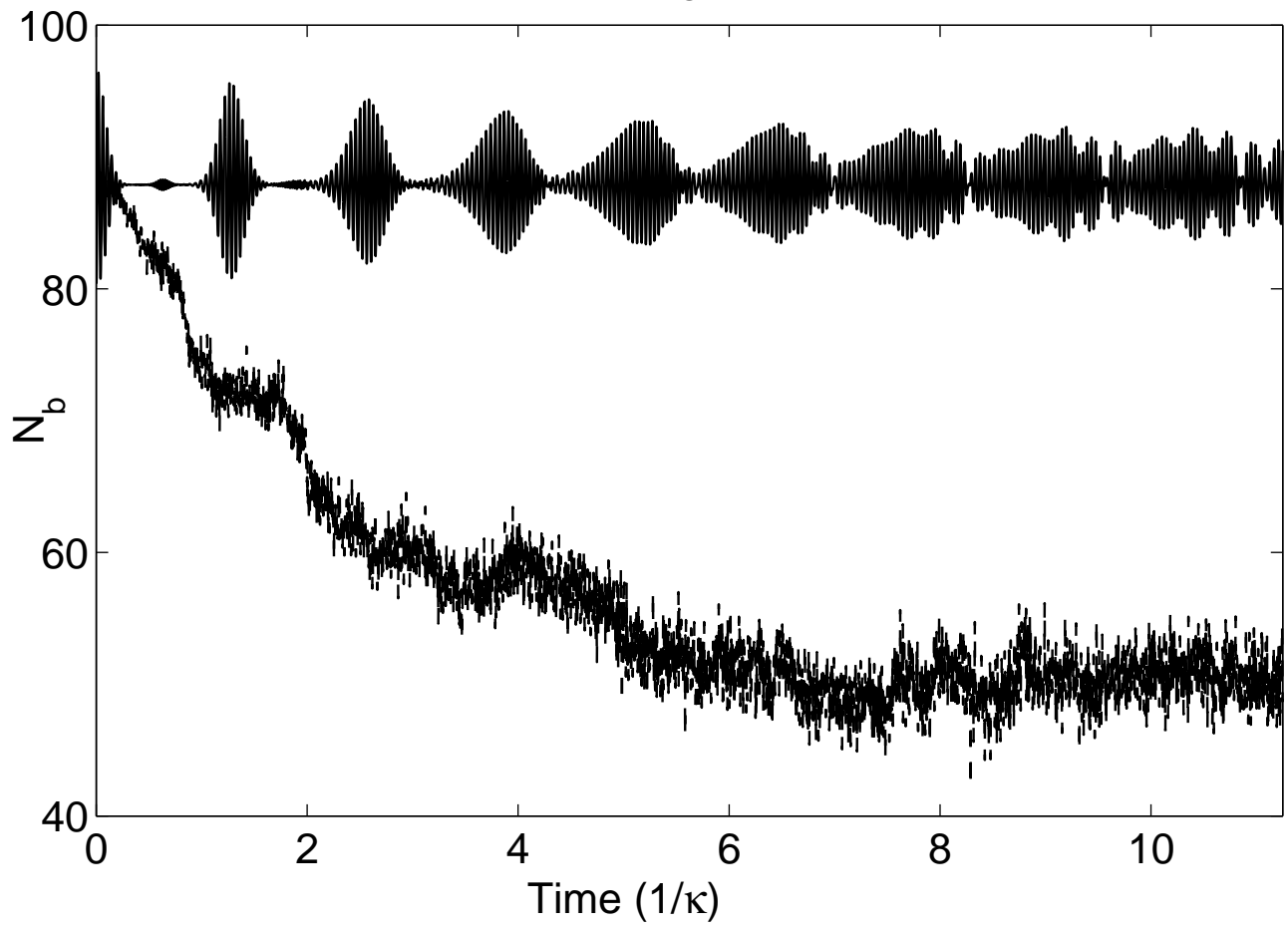


Fig.3a

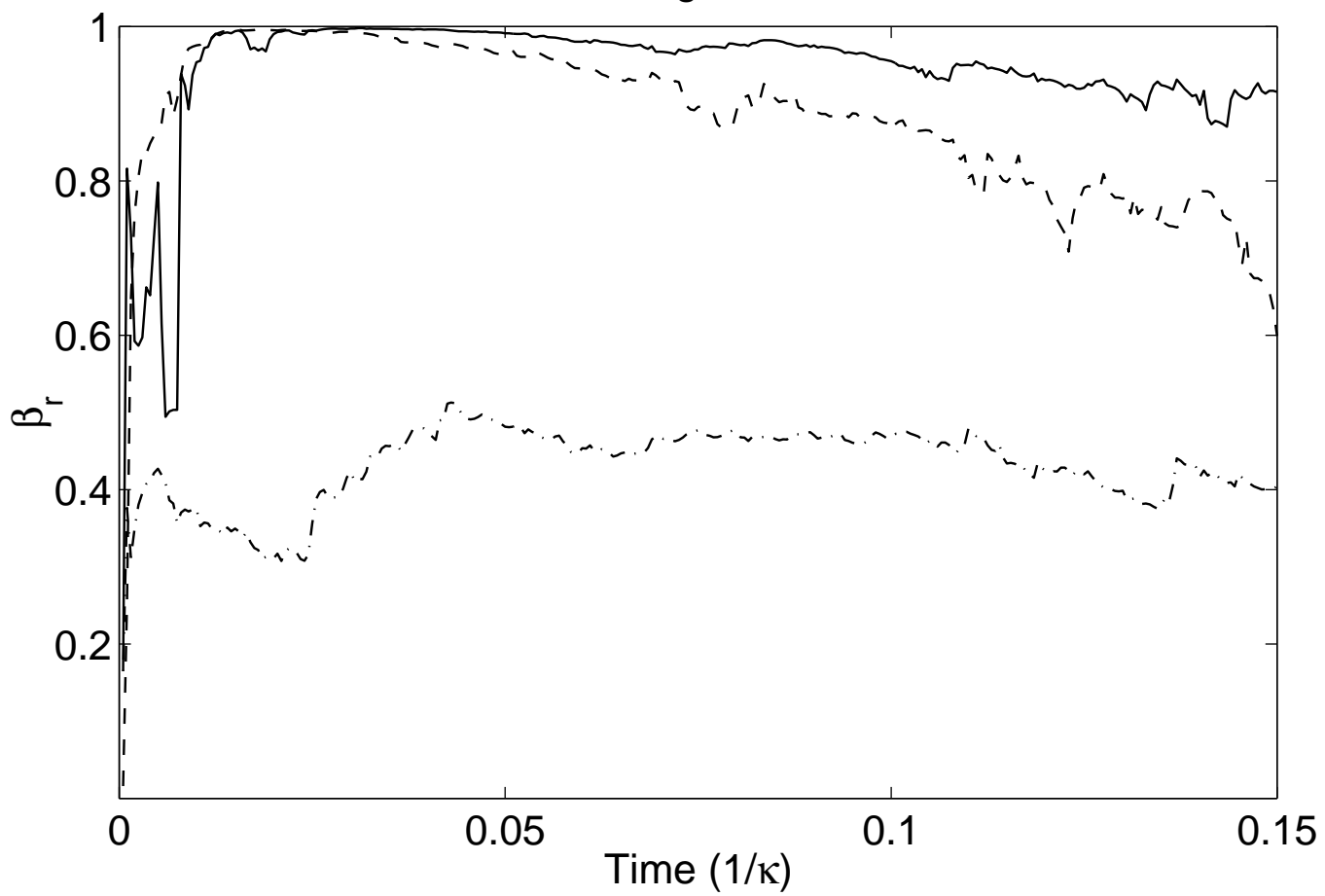


Fig.3b

